Journal of Nuclear Medicine, published on December 4, 2020 as doi:10.2967/jnumed.120.255679

Phase I trial of ^{131}I-GMIB-Anti-HER2-VHH1, a new promising candidate for HER2-targeted radionuclide therapy in breast cancer patients

Matthias D'Huyvetter[1,2], Jens De Vos[1], Vicky Caveliers[2,3], Ilse Vaneycken[3], Johannes Heemskerk[3], Francois P. Duhoux[4], Christel Fontaine[5], Marian Vanhoeij[6], Albert D. Windhorst[7], Frank van der Aa[7], N. Harry Hendrikse[7], Jos L.E. Eersels[1,2], Hendrik Everaert[3], Pieterjan Gykiere[3], Nick Devoogdt[1,2], Geert Raes[1,8,9], Tony Lahoutte[1,2,3], Marleen Keyaerts[2,3]

[1]Precirix NV/SA, Brussels, Belgium

[2]In Vivo Cellular and Molecular Imaging Laboratory (ICMI), Vrije Universiteit Brussel, Belgium

[3]Nuclear Medicine Department, UZ Brussel, Belgium

[4]Medical Oncology Department, King Albert II Cancer Institute, Cliniques universitaires Saint-Luc, and Institut de Recherche Expérimentale et Clinique, Université Catholique de Louvain, Brussels, Belgium

[5]Department of Medical Oncology, UZ Brussel, Brussels, Belgium

[6]Department of Oncological Surgery, UZ Brussel, Brussels, Belgium

[7]Amsterdam UMC, Vrije Universiteit Amsterdam, Department of Radiology & Nuclear Medicine, Amsterdam, The Netherlands

[8]Lab of Cellular and Molecular Immunology, Vrije Universiteit Brussel, Brussels, Belgium

[9]Myeloid Cell Immunology Lab, VIB Center for Inflammation Research, Brussels, Belgium

Corresponding author: Marleen Keyaerts, Laarbeeklaan 103, B-1090 Brussels, 0032-2-477-50-20, marleen.keyaerts@vub.be

First author: Matthias D'Huyvetter, Precirix NV/SA, Burgemeester Etienne Demunterlaan 1, B-1090 Brussels, 0032-2-479-93-60, Matthias.dhuyvetter@precirix.com

Financial support: Marleen Keyaerts and Tony Lahoutte are Senior Clinical Investigators of the Research Foundation–Flanders. Francois Duhoux received a postdoctoral clinical mandate (2017-034) from Foundation Against Cancer. Research was funded by Innoviris.Brussels (RBC/2014-R-75).

Word count: 6729

Running title: ^{131}I-GMIB-Anti-HER2-VHH1 in HER2-therapy

Key words: single domain antibody, Iodine-131, breast cancer, theranostics

ABSTRACT

Introduction: ^{131}I-GMIB-Anti-HER2-VHH1 is a targeted radionuclide theranostic agent directed at HER2 expressing cancers. VHH1 is a single domain antibody fragment covalently linked to therapeutic radio-iodine ^{131}I via the linker SGMIB. The Phase I study presented was aimed at evaluating the safety, biodistribution, radiation dosimetry and tumor imaging potential of ^{131}I-GMIB-Anti-HER2-VHH1 in healthy volunteers and breast cancer patients.

Methods: In a first cohort, six healthy volunteers were included. The biodistribution of ^{131}I-GMIB-Anti-HER2-VHH1 was assessed using whole body (anterior and posterior) planar images obtained at 40 min., 2, 4, 24 and 72 h following i.v. administered (38 ± 9 MBq) ^{131}I-GMIB-VHH1. Imaging data were analyzed using OLINDA/EXM software 1.0 to determine the dosimetry. Blood and urine samples were obtained over 72h.

In the second cohort, three patients with metastatic HER2 positive breast cancer were included. Planar whole-body imaging was performed at 2 h and 24 h after injection. Additional SPECT/CT images were obtained following the whole body images at 2 and 24 h in case of relevant uptake in known cancer lesions

Results: No drug related adverse events (AEs) were observed throughout the study. The biological half-life of ^{131}I-GMIB-Anti-HER2-VHH1 in healthy subjects was about 8 h. After i.v. administration, the compound is eliminated from the blood with a 2.5 h half-life. The drug is primarily eliminated via the kidneys. The drug was stable in circulation and there was no increased accumulation in thyroid or stomach. The absorbed dose to the kidneys was 1.54 ± 0.25 mGy/MBq, while to bone marrow 0.03 ± 0.01 mGy/MBq. SPECT/CT imaging in patients with advanced breast cancer showed focal uptake of ^{131}I-GMIB-Anti-HER2-VHH1 in metastatic lesions.

Conclusion: No AEs were observed after iv administration of ^{131}I-GMIB-Anti-HER2-VHH1 at low activity. Unbound drug is rapidly eliminated via the kidneys. In patients with stage IV HER2 positive

breast cancer accumulation of ^{131}I-GMIB-Anti-HER2-VHH1 in metastatic sites was observed. Dosimetry predicts kidneys as the dose limiting organ upon dose escalation, but kidney toxicity should only occur at very high injected activities. Dose escalation is planned in a subsequent phase I/II study to assess the therapeutic window of this compound (NCT04467515).

INTRODUCTION

Single domain antibodies (sdAbs), VHHs or nanobodies, are the antigen-binding units derived from natural light-chain-deficient camelid antibodies. Compared to conventional antibodies and their antibody fragments, sdAbs are smaller (15 kDa) and can bind antigens on hidden or unusual epitopes. sdAbs are considered low immunogenic, have nanomolar affinities and can be produced in high yields (1,2).

Tumor cell membrane antigens represent an important target for anti-cancer treatment. Theoretically, sdAbs can be generated against virtually any cancer-specific membrane-associated protein such as for example HER2 or CD20, and bear unusually beneficial properties for targeted radionuclide therapy (TRNT) (3-8). The human epidermal growth factor receptor type 2 (HER2) is a typical example of a membrane receptor that may be overexpressed on the cell membrane of breast, ovarian and gastric carcinoma (9). Activation of this receptor stimulates cancer cell proliferation, resulting in increased cell mobility and less apoptosis. Consequently, HER2 overexpression is associated with tumor aggressiveness and an increased probability for recurrent disease. Targeted therapies for HER2 are clinically used, such as monoclonal antibodies (trastuzumab and pertuzumab) that specifically bind the extracellular domain of HER2, specific tyrosine kinase inhibitors (lapatinib) that interact with the intracellular domain of HER2, or antibody-drug conjugates derived from monoclonal antibodies. Information on the HER2 status of tumors is therefore of major importance since it has an enormous impact on the therapy selection. At present, HER2 expression is assessed using tissue biopsies. However, even with such patient selection, treatment failure still occurs, either immediately or via acquired resistance. New-generation anti-HER2 agents, such as antibody-drug conjugates, have shown therapeutic efficacy in patients in whom antibody-based or TKI-based therapy regimens already failed, exemplifying the potential of improved HER2 treatment agents.

Anti-HER2-VHH1, also referred to as sdAb 2Rs15d, targets HER2-receptor and was selected as a lead compound because of superior characteristics and the fact that it does not compete with binding of trastuzumab and pertuzumab (10). In its radionuclide therapy formulation, it introduces a novel mechanism of action to the landscape of HER2-targeted treatments.

^{68}Gallium-labelled anti-HER2-VHH1 (^{68}Ga-NOTA-HER2) is under clinical development for the detection of HER2 expression in known tumoral sites using PET. A first-in human trial in 20 breast cancer patients using this tracer was successfully conducted (11,12), and multiple phase II trials are ongoing. No treatment-related adverse events (AEs) were observed. The main conclusions were that (i) ^{68}Ga-DOTA-HER2 PET/CT is a safe procedure with radiation doses comparable to other PET/CT procedures and (ii) imaging reveals whole-body expression of HER2 in primary tumors and metastases.

Preclinical studies with ^{131}I-labeled Anti-HER2-VHH1 (^{131}I-GMIB-Anti-HER2-VHH1) were conducted evaluating the potential of this compound as a therapeutic agent for TRNT. In these preclinical studies, the compound revealed similar tumor targeting characteristics and in vivo blood clearance compared to the ^{68}Ga-labeled compound. Surprisingly, the biodistribution profile for ^{131}I-GMIB-Anti-HER2-VHH1 was more favorable with much lower kidney uptake values compared to ^{68}Ga-NOTA-HER2. The absorbed dose delivered to the tumor remained high and was higher than the to kidney. This favorable biodistribution, combined with the theranostic characteristics of ^{131}I, has now triggered the interest to use this compound as a potential TRNT agent in metastatic patients with HER2-positivity (13). ^{131}I- GMIB-Anti-HER2-VHH1 at low injected activity could be used for confirming accumulation in HER2 positive disease, followed by a number of cycles with ^{131}I-GMIB-Anti-HER2-VHH1 at high injected activity for therapy. Here we present the first-in-human results with low injected activity ^{131}I-GMIB-Anti-HER2-VHH1 to assess safety,

tolerability, biodistribution, dosimetry and tumor uptake in healthy volunteers and in HER2-positive breast cancer patients.

MATERIALS AND METHODS

Preparation of ^{131}I-GMIB-Anti-HER2-VHH1

All reagents and solvents were obtained from commercial suppliers and were HPLC-grade or analytical grade and used as such. N-Succinimidyl 4-[N^1,N^2-Bis(Boc)guanidino-methyl]-3-trimethylstannyl)benzoate (precursor for iodination) and SGMIB (N-Succinimidyl 4-guanidino-methyl-3-iodobenzoate) as reference standard were obtained from ABX Chemicals (Radeberg, Germany) in freeze-dried 50 µg aliquots. Radioiodide ($Na^{131}I$, no carrier added; specific activity of > 55.5 GBq/µmol) in 0.05 M NaOH was obtained from GE Healthcare, Germany.

To obtain ^{131}I-SGMIB, 0.20 mL of 2% HOAc in ACN, 50 µg SGMIB precursor dissolved in 0.10 mL ACN and N-chlorosuccinimide (400 µg) in 50 µL ACN were added to 50 µL of Na[^{131}I]I-solution (1,924 ± 273 MBq) and reacted for 15 min at room temperature. After labelling, the reaction mixture was dried at 50°C under a gentle N_2-flow. For removal of the Boc-protecting groups 0.15 mL trifluoroacetic acid (TFA) was added and allowed to react for 15 min. After deprotection, traces of TFA were removed from the deprotected reaction mixture by adding 0.10 mL ACN and subsequently followed by evaporation. To the dried ^{131}I-SGMIB, 2.0 mL eluent was added and injected on HPLC for semi-preparative HPLC-purification of ^{131}I-SGMIB. Semi-preparative HPLC-purification consisted of the following components and parameters: 2.0 mL/min, a 19/81 ACN/4 mM NaH_2PO_4 mobile phase, a Symmetry RP-18 (Waters Milford, US) 300x7.8 mm, 7 µm column, UV wavelength 254 nm. The collected ^{131}I-SGMIB was further concentrated by means of a SPE cartridge (tC18 Plus, Waters, preconditioned with 5 mL ACN and 10 mL of water) and eluted in 1.0 mL 1% HOAc/ACN. ^{131}I-SGMIB was obtained in a radiochemical yield of 32.2 ± 7.4 %.

Purified ^{131}I-SGMIB was dried and 0.10 mg Anti-HER2-VHH1 in 0.10 mL 0.1 M borate buffer (pH 8.5) was added for conjugation during 25 min. The conjugated reaction mixture was diluted with 0.7 mL formulation buffer (5 mg/mL ascorbic acid in 0.9% NaCl pH 5.2) and loaded on a PD-10 column for purification. Another 2.0 mL of formulation buffer was added and discarded. ^{131}I-GMIB-Anti-HER2-VHH1 was collected by eluting with 3.0 mL of formulation buffer.

A panel of analytical tests was included: visual inspection, pH, radiochemical purity, binding affinity, sterility filter membrane integrity test, bacterial endotoxins and sterility. All analytical procedures are validated and adequate to detect significant deviations from the specifications. In short, visual inspection was performed after final sterile filtration to confirm that the solution is clear and colorless. The pH of the drug product was determined by pH electrode. Radiochemical purity was performed using instant thin-layer chromatography (iTLC) and size exclusion chromatography, equipped with UV and radioactivity detection. As eluent for iTLC 20 mM citric acid with 10% of acetonitrile was used. In parallel, analysis via size exclusion chromatography (SEC) was executed and consisted of the following components and parameters: 0.75mL/min, 50 mM sodium phosphate, 0.15 M NaCl, 10 mM NaN_3 pH=6.6, GE Superdex Peptide 10/300 GL, run time of 60 min, UV wavelength 280 nm. Endotoxin levels were assessed by use of an FDA-licensed LAL test system according to the instructions provided by the supplier (Endosafe®-PTS, Charles River). The filter integrity test is performed according to the bubble-point method, according to Ph. Eur. The integrity of the sterile end-filter is tested as part of the manufacturing process. Sterility testing was performed according to Ph. Eur on a non-radioactive media fill. Antigen binding was assessed through the Lindmo assay using $HER2^+$ SKOV-3 cells. The incubation was done overnight at room temperature on a shaking device.

Study design and approvals

This was a single center, open label, non-randomized first-in-human clinical trial. The trial design is depicted in Figure 1. The study was approved by the Belgian federal agency for medicines and health products (FAMHP), the regional ethics committee of UZ Brussel and the radiation protection agency of Belgium (FANC), and registered with the identifiers EudraCT 2015-004840-21 and NCT02683083. The study was conducted in accordance with the Declaration of Helsinki and the International Conference on Harmonization Guidelines for Good Clinical Practice. Written informed consent was obtained from all participants.

The study was performed in 2 parts, with in part I inclusion of 6 healthy volunteers. After approval by the independent Data Safety Monitoring Board, 3 breast cancer patients were included in part II to assess uptake of ^{131}I-GMIB-Anti-HER2-VHH1 in metastatic lesions.

Study population, inclusion and thyroid blockage

Six healthy Caucasian volunteers (5 females, 1 male) were included to assess safety, biodistribution and dosimetry and three breast cancer patients (2 females, 1 male, aged ≥18 years) were included to assess uptake of in metastatic lesions.

Patients with local, locally advanced or metastatic HER2+ breast carcinoma (defined as either immunohistochemistry score of 3+ or in situ hybridization (ISH) amplified) were included.

Key exclusion criteria for both subgroups were pregnancy or lactation, contra-indication for thyroid blockage with potassium iodine, abnormal liver function (ALT/AST > 2 times upper limit of the normal (ULN); bilirubin > 1.5 times ULN) or kidney function (eGFR < 50 ml/min/1.73 m^2), serious active infection, recent gastro-intestinal disorder with diarrhea, other life-threatening illness, inability to communicate reliably or give informed consent, patients unlikely to cooperate with the requirements of the study or patients who already participated in this study or a previous

study with anti-HER2 VHH1. In addition, healthy volunteers were excluded in case of clinically significant disease or previous thyroid disorders. For part II, patients with at least 1 lesion of minimal 15 mm diameter were studied to assess uptake of ^{131}I-GMIB-Anti-HER2-VHH1 in metastatic lesions.

Study medications

For thyroid blockage, 130 mg potassium iodide was daily administered orally for 4 consecutive days starting 24 h before the administration of ^{131}I-GMIB-Anti-HER2-VHH1. The dose range in the study protocol was a single dose continuous infusion of 50 ± 40 µg with a radioactivity range of 46 ± 28 MBq for healthy subjects and 64 ± 46 MBq for patients. The radiopharmaceutical was administered over 5 min via a peripheral intravenous line using an infusion pump. The empty syringe and intravenous line were measured for residual radioactivity after injection. The subjects did not void until after completion of the first whole body planar scan. All subjects were fasted for at least 4h before receiving the dose.

Safety assessment

Vital parameters (blood pressure, heart rate and temperature) were monitored throughout the study. Hematologic and metabolic panels (hemoglobin, white blood cells, neutrophils, lymphocytes, platelets, creatinine, blood urea nitrogen, calcium, sodium, potassium, carbon dioxide, lactate dehydrogenase, alanine transaminase, aspartate aminotransferase, alkaline phosphatase, total bilirubin, and albumin), were obtained prior to administration, and at 24 h after injection of ^{131}I-GMIB-Anti-HER2-VHH1. Subjective adverse events (AEs) were assessed using open questions before injection, throughout the time that subjects were present in the nuclear

medicine department, and at subsequent visits up to 24 h after injection for patients and up to 72 h after injection for healthy volunteers.

Planar and SPECT/CT imaging

Images were acquired using a Philips BrightView XCT equipped with high-energy general purpose (HEGP) collimators, photopeak was set at 364 keV (20% window, scatter windows of 6%). Whole-body images were acquired at 10 cm/min. The matrix size was 512 by 1024 pixels; pixel size was 2.8 mm. Whole-body images were acquired at 40 min, 2 h, 4 h, 24 h and 72 h in healthy volunteers and at 15 min, 2 h and 24 h in patients.

During whole body image acquisition, a source of known activity of ^{131}I was positioned between the lower legs of the subject. Distance between camera bed and each camera head was kept constant for each subject. In healthy volunteers, dynamic acquisitions over liver and kidneys were acquired during injection up to 30 min after start of injection.

SPECT/CT was optional after whole-body imaging at 2 h and 24 h in patients, and was decided by the primary investigator based on uptake in known cancer lesions. SPECT/CT acquisitions consisted of 64 projections of 40 sec, in step-and-shoot mode, with a matrix of 128 by 128 pixels of 4.7 mm. Scatter was corrected by scaled subtraction of the scatter window projection images before reconstruction, reconstruction was performed using manufacturer's proprietary iterative reconstruction algorithm (Astonish) (14). Reconstructed images had 4.7 mm isotropic voxels. CT images were acquired (120 kV,80 mA) for localization and attenuation correction.

Blood and urine samples

Pharmacokinetics in the blood were assessed using radioactive counting of blood and plasma samples over time. In healthy volunteers, blood samples were taken from a peripheral vein before

injection, at 5, 10, 30, 60, 105 and 225 min, and at 24 h and 72 h post injection. Urine sample were collected at about 60 and 225 min, and at 24 h and 72 h p.i. Whole blood and plasma samples were counted against appropriate standards of known dilution in an automatic gamma well counter and, after correction for decay and background activity, expressed as a percentage of the injected activity (%IA). The blood volume of each volunteer was estimated according to body weight and height, using Nadler's formula and the patient's hematocrit. Blood half-lives were calculated with a two-phase exponential decay model using GraphPad Prism software (GraphPad Software, La Jolla, CA, USA).

Plasma of pre-selected time points and urine aliquots of five healthy volunteers and three patients were analyzed by size-exclusion chromatography or reversed phase-high performance liquid chromatography to identify possible metabolites. The HPLC system consisted of a Hitachi Chromaster (VWR Belgium) equipped with a Pump with a low-pressure gradient system, a 6-channel degasser, a manual injector, a Flowstar LB513 radioactive detector (Berthold, Germany) and a Hitachi Chromaster UV detector. Data acquisition was performed using the Flowstar software.

Each sample was injected on a Superdex 75 (GE Healthcare) 5/150 GL column at room temperature. The mobile phase consists of 50 mM sodiumphosphate, 0.15 M NaCl and 0.01 M NaN_3. Analysis was carried out at a flow rate of 0.3 ml/min with an isocratic program using a 20 min run time.

Region-of-interest Definition and Dosimetry

The uptake of ^{131}I-GMIB-Anti-HER2-VHH1 in different organs was determined from anterior and posterior whole-body images (by calculating the geometric mean). ROIs were drawn (whole-body, brain, lungs, liver, kidneys, thyroid, heart, intestines, bladder, thigh muscle) using Osirix software

(Pixmeo SARL, Switzerland). For dosimetry calculations, OLINDA/EXM software 1.0 (Organ Level Internal Dose Assessment/EXponential Modeling, Vanderbilt University) *(14)* was used. A bi-exponential fit was used, excretion parameters were set at 95% for renal excretion, and 4.8 h for the voiding bladder interval. Both male and female adult models were applied on every healthy subject, regardless of the sex of the subject. Averages of all six healthy volunteers are reported per sex.

RESULTS

Preparation of ^{131}I-GMIB-Anti-HER2-VHH1

The radiopharmaceutical was produced at Amsterdam UMC, (VUmc) according to cGMP guidelines. ^{131}I-GMIB-Anti-HER2-VHH1 (n = 9) was obtained in a yield of 6.1 ± 1.7% calculated from Na^{131}I with an average total synthesis time of 3 h 44 min ± 28 min. One batch contained 83 ± 20 MBq of ^{131}I-GMIB-Anti-HER2-VHH1 in a sterile, isotonic and pyrogen free solution for i.v. injection. pH of the final drug product solution ranged 5.2 – 5.6. ^{131}I-GMIB-Anti-HER2-VHH1 was obtained at molar ratio (^{131}I-SGMIB)-to-(sdAb) of (0.09 ± 0.02) - to - (1.0). Radiochemical purity (RCP) after synthesis (n = 9) measured 97.8 ± 3.2% via instant thin layer chromatography (iTLC) and 99.7 ± 0.5% size-exclusion chromatography (SEC), while the Lindmo assay revealed an immunoreactive fraction of 73.9 ± 9.5%. After 24 h, RCP calculated 96.4 ± 2.5% (iTLC) and 97.4 ± 1.4% (SEC). The mean administered activity of ^{131}I-GMIB-Anti-HER2-VHH1 was 38.1 ± 8.8 MBq (range 24.7 - 49.7 MBq) for healthy volunteers, and 60.7 ± 4.3 MBq (range 56.9 - 65.3 MBq) for patients, with a protein amount ranging 10-90 µg anti-HER2 VHH1 for all participants.

Subject characteristics, safety and tolerability

All subjects were fully compliant with the oral intake of potassium iodide for thyroid blockade. Subject demographics are provided in Supplemental Table 1. In healthy volunteers, four AEs of mild intensity were recorded (ecchymosis, adhesive plaster sensitivity, abdominal discomfort). In patients, no adverse events (AEs) were noted. All AEs were considered unrelated or unlikely related to the study drug. There were no adverse drug reactions or clinically-detectable pharmacological effects in any of the 9 subjects. No significant changes in vital signs or laboratory parameters were observed.

Dynamic, whole-body imaging in healthy subjects

Given the fast pharmacokinetics of sdAbs, dynamic imaging of the upper abdomen was performed (30 images of 1 min each) to evaluate the initial kidney activity. Representative images and relative mean time-activity curves are shown in Supplemental Figure 1. Although absolute kidney uptake varies between subjects, the dynamics are very reproducible over all 6 investigated subjects. An initial fast uptake is seen over the first 10 min, followed by a slow increase.

Representative whole-body images of a healthy volunteer 40 min – 24 h after injection are shown in Figure 2. Geometric mean images of all other subjects are shown in Supplemental Figure 2. The most intense uptake is visible in kidneys, and in a variable degree in liver. Faint uptake is observed in salivary glands and intestines. In all subjects, faint activity in the region of the colon can be seen at 24 h after injection (Supplemental Figure 3), indicating a minor level of gastro-intestinal uptake and/or excretion. No uptake is visible in thyroid or stomach (as expected due to blockade by potassium iodide), brain, muscle or normal breast tissue. Uptake in organs was measured using five whole body imaging time points, and average uptake values are shown in Supplemental Table 2.

Whole body clearance over 72 h was calculated based on the activity remaining in the body of healthy volunteers, excluding any bladder activity, over time. Using a mono-exponential curve fit, the biological half-life was calculated from these data for each healthy subject and was on average 7.72 ± 1.40 h (Figure 3).

Blood and urine sample analysis in healthy subjects

On average 97.48 ± 1.85% of ^{131}I-GMIB-Anti-HER2-VHH1 was in the plasma fraction at 60 min after injection. The blood clearance in healthy volunteers is shown in Figure 4. A bi-exponential curve fit resulted in a distribution phase to the tissues with a mean half-life of 6.70 ± 1.13 min and an elimination phase from the body with a half-life of 150.80 ± 35.69 min. For one subject, the sample obtained at 10 min was omitted for this analysis because it revealed a higher value than the sample at 5 min, and this was considered a procedural error.

Metabolites were analyzed in blood of healthy subjects at 5 different time points. On a total of 30 samples there was only one sample that showed a measurable metabolite peak on HPLC analysis. It was a blood sample at 1 h after injection, with no detectable metabolites in the subsequent blood samples at 4 h, 24 h and 72 h after injection. In order to further substantiate the absence of metabolites in blood, additional metabolite analysis was performed in the subsequent 3 patients. No metabolites were detected in these patients' samples 1 h after injection. In urine samples, up to three different metabolites were detected until 24 h in all subjects and in one subject until 72 h after injection. Further identification of metabolites was not part of this study.

Region-of-interest definition and dosimetry in healthy subjects

Dosimetry values for individual organs as well as whole-body estimated absorbed dose are shown in Table 1 as average of 6 healthy volunteers. The organs showing the highest absorbed doses

were the kidneys, followed by the urinary bladder wall and the lower large intestine. The absorbed dose to the kidneys is 1.63 mGy/MBq in female subjects. The bone marrow absorbed dose of 0.038 mGy/MBq in females is low.

Tumor uptake in Cancer Patients

Patient 1. 43-year-old male, recent diagnosis of metastatic (bone) estrogen receptor-positive and HER2-positive breast cancer. The patient had started a first-line treatment with trastuzumab – pertuzumab – docetaxel and he had received the 2nd cycle 8 days prior to ^{131}I-GMIB-Anti-HER2-VHH1 injection. Focal uptake was seen at the site of a 33 mm (largest axis) bone metastasis in the right acetabulum (Figure 5). Treatment was continued resulting in a partial metabolic response on ^{18}F-FDG PET/CT imaging after the 4th cycle.

Patient 2. 77-year-old woman with a recent history of ER-positive HER2-positive breast cancer and a metastasis in the sternal bone. Her first evaluation under treatment with trastuzumab – pertuzumab – paclitaxel showed progressive disease with extension of the sternal lesion to the clavicular bone and the first left rib, as well as new liver metastases (all liver metastases < 15 mm in size). Two days after the last mAb treatment, she participated in this clinical trial. After injection of ^{131}I-GMIB-Anti-HER2-VHH1, the planar whole-body scan and SPECT/CT showed focal uptake in the large sternal metastasis, persisting until 24 h after injection (Figure 6). Uptake in this sternal lesion was calculated using ROI analysis on planar imaging as 1.6 %IA at 2 h.

Patient 3. 61-year-old woman with ER-positive HER2-positive breast cancer. She was receiving a first-line treatment with paclitaxel - trastuzumab - pertuzumab for distant lymph node invasion in mediastinum and retroperitoneum and pleural disease at time of inclusion. Planar whole-body imaging with ^{131}I-GMIB-VHH1, administered 21 days after trastuzumab-pertuzumab injection, did not show lesional uptake. On SPECT/CT, only faint tracer accumulation is visible in subcarinal

lymph node and in pleural metastasis (Figure 7).

DISCUSSION

TRNT is an attractive therapeutic modality wherein a labeled targeting moiety selectively targets cancer cells and may deliver a lethal payload from a decaying radionuclide. However, intact antibodies might not be ideal vectors due to their large size (~150 kDa), resulting in suboptimal pharmacokinetics, poor tumor penetration, and slow normal-tissue clearance (15). Efforts to optimize pharmacokinetics of larger vectors, such as pre-targeting, are gaining more attention. Due to their high specificity of binding, sub-nanomolar affinity, and low immunogenicity, sdAbs are attractive probes for imaging and radionuclide therapy. Their small size (10–15 kDa) facilitates tumor penetration and rapid elimination from blood and normal tissues compared to intact antibodies (16). SdAbs have been directed to a variety of transmembrane cancer cell molecular targets to image and/or treat cancer in (pre-)clinical models of breast (12,13) and ovarian cancer (5), multiple myeloma (4) and non-Hodgkin lymphoma (6).

The rationale for clinical translation of ^{131}I-GMIB-Anti-HER2-VHH1 is fivefold: (i) the use of ^{131}I-SGMIB as a prosthetic group results in a stable drug product in vivo, with no associated dehalogenation as compared to iodogen based direct radioiodination methods (17); (ii) preclinical studies have indicated that ^{131}I-GMIB-Anti-HER2-VHH1 at high injected activity has a therapeutic effect while accumulation in kidneys significantly lower compared to radiometal-based analogs (5,13); and (iii) HER2-targeting VHH1 targets a unique epitope and does not compete with trastuzumab and pertuzumab, which allows the use of ^{131}I-GMIB-VHH1 in patients who undergo HER2-targeted therapies (10,13), (iv) because ^{131}I-GMIB-Anti-HER2-VHH1 brings a novel mechanism of action to the field of HER2-targeted therapeutics, and (v) the theranostic

character with low injected activity radioiodine or PET-labels such as ^{68}Ga /^{18}F to select patients based on imaging, who are likely to benefit from high injected activity treatments (18).

This first-in-human application of the radioiodinated sdAb ^{131}I-GMIB-Anti-HER2-VHH1 demonstrated no drug-related AE in healthy volunteers or patients at low injected activities. The radiopharmaceutical was well tolerated by all study subjects. There were no clinically relevant changes in vital signs, physical examination or blood parameters. The biological half-life of ^{131}I-GMIB-Anti-HER2-VHH1 was about 8 h. More than 95% of the drug was present in the plasma fraction of blood with a fast plasma elimination half-life of 2.5 h, and did not show general trends of metabolization in blood. The consistent presence of metabolites in urine indicate renal metabolization. The product specifications obtained prior to i.v. injection confirmed that no significant free iodine was injected.

^{131}I-GMIB-Anti-HER2-VHH1 showed a favorable biodistribution and is primarily eliminated via the kidneys and only to a minor extent via the intestinal tract. At 40 min after i.v. injection, on average 24% ^{131}I-GMIB-Anti-HER2-VHH1 is in the kidney and 14% is in the liver. The washout from these organs is fast with only 4% in kidney and 2% in liver at 24h. Thyroid or stomach showed no specific accumulation, which was expected as patients were pre-treated with potassium iodide for blockage.

^{131}I-GMIB-Anti-HER2-VHH1 proved to be safe after a single injection of a drug with protein amount ranging 10-90 mg and an average injected activity of 60.7 MBq (range: 24.7- 65.3 MBq). Dosimetry analysis predicts that the dose-limiting organ will be the kidney, receiving the highest absorbed dose of 1.62 mGy/MBq. As described by Santoro and colleagues, no clear cumulative absorbed dose cut-off has been identified in Peptide Receptor Radionuclide Therapy (PRRT) with ^{177}Lu to predict the risk of organ failure. Reports often refer to 23 Gy for kidneys and 2 Gy for bone marrow, although these values are obtained with fractionated EBRT (19). The administration

of 15 GBq would lead to an absorbed dose to kidneys of 23 Gy. Bone marrow is the most radiosensitive tissue in the body. ^{131}I-GMIB-Anti-HER2-VHH1 results in a low-level bone marrow exposure (0.038 mGy/MBq). This level of irradiation would only occur after administration of 59.0 GBq ^{131}I-GMIB-Anti-HER2-VHH1. Therefore, kidney- and hematotoxicity are unlikely to occur in the planned dose escalation study of ^{131}I-GMIB-Anti-HER2-VHH1 (1.85 – 7.4 GBq). ^{131}I-GMIB-Anti-HER2-VHH1 at an injected activity of 7.4 GBq would deliver absorbed doses to kidneys and to bone marrow well below the defined levels of 23 Gy for kidneys and 2 Gy for bone marrow, as typically accepted by regulatory agencies for therapeutic radiopharmaceuticals. It is important to note that the current study was performed without kidney protection measures such as arginine/lysine infusion before and after drug administration, a method routinely used in PRRT (e.g. ^{177}Lu-DOTATATE (Lutathera®, Novartis)). Preclinical studies with radiolabeled sdAbs show that the administration of gelofusine or positively-charged amino acids can reduce kidney retention levels by more than 40% (5,20). Consequently, introduction of this amino acid infusion before and after drug administration could potentially double the maximal tolerable dose.

As a secondary objective in this Phase I study, tumor uptake was evaluated in three patients with HER2-positive breast cancer. Uptake was clearly present in two patients with lesions above 3 cm, and in a third patient with smaller lesions, low-level uptake could be visualized, likely because of partial volume effects. The strongest uptake was seen in a patient with progressive disease at the time of study drug administration. In patient 1, a known bone metastasis in the right acetabulum above 3 cm was visualized on planar and SPECT/CT images at both early time points after injection as well as after 24 h. In patient 2, focal uptake was observed in a known bone metastasis in the sternum of more than 3cm through total body scans and in SPECT/CT images taken at 2 and 24 h. The focal drug accumulation in the cancer lesion showed a sharp contrast with surrounding tissues. Patient 3 had no lesions above 3 cm and only low-level uptake

was identified by visual interpretation of the scan. The therapeutic value of this compound will be assessed in the planned phase I/II dose escalation and expansion study (NCT04467515). Centralized production through an optimized process will allow for a steady supply of ^{131}I-GMIB-Anti-HER2-VHH1 to multiple clinical sites that take part in this study.

We previously described the preclinical evaluation of ^{131}I-GMIB-Anti-HER2-VHH1. Here it was shown that ^{131}I-GMIB-Anti-HER2-VHH1 is cleared fast in mice via kidneys, with only minor activity in liver (13). The data presented herein indicate that the biodistribution and pharmacokinetic data in human are very similar to the data predicted from preclinical experiments. I Its optimal biodistribution in combination with its proven preclinical efficacy in models of breast and ovarian cancer forms the basis for further clinical investigation of ^{131}I-GMIB-Anti-HER2-VHH1. Moreover, it was recently shown that treatment with ^{131}I-GMIB-Anti-HER2-VHH1 showed improved survival over trastuzumab in a preclinical model of HER2+ brain metastases. Indeed, these results indicate that the small size of sdAbs allows more efficient targeting beyond the breached blood-brain-barrier compared to full-size antibodies such as trastuzumab (21).

CONCLUSION

The here-presented human data of a radioiodinated sdAb for therapeutic intent support the translational potential of radiolabeled sdAbs in general and ^{131}I-GMIB-Anti-HER2-VHH1 in particular, beyond imaging purposes. Dosimetry predicts kidneys as the dose limiting organ upon dose escalation, but kidney toxicity should only occur at very high injected activities. The uptake in HER2-positive lesions further supports its therapeutic potential and opens new therapeutic options for patients who progress on trastuzumab, pertuzumab or T-DM1, given its distinct mode-of-action. The results of this study prompted a multi-center dose escalation and therapeutic

clinical investigation (NCT04467515) of ^{131}I-GMIB-Anti-HER2-VHH1 in patients with HER2 positive breast and gastric cancer.

DISCLOSURES

G. Raes, N. Devoogdt and T. Lahoutte are consultants for Precirix NV/SA and together with M. D'Huyvetter and J. De Vos hold ownership interest in Precirix NV/SA. M. Keyaerts, G. Raes, N. Devoogdt and T. Lahoutte hold ownership interest in Abscint NV/SA. T. Lahoutte is member of the scientific advisory board of Ion Beam Applications (IBA) and member of the strategic committee of the Institute of RadioElements (IRE). M. Keyaerts has received travel and accommodation expenses from Bayer NV. N. Devoogdt has received funding for preclinical research from Boehringer-Ingelheim, Complix, Confo Therapeutics, Roche, 121BIO, Agenus and Telix Pharma. M. Keyaerts, N. Devoogdt, M. D'Huyvetter, J. De Vos, T. Lahoutte and G. Raes have patents on sdAb imaging and therapy.

F.P. Duhoux holds Advisory/Consultancy roles for Amgen, AstraZeneca, Daiichi Sankyo, Eli Lilly, Novartis, Pfizer, Pierre Fabre, Roche and Teva (paid to institution, outside the submitted work). Speaker fees for Eli Lilly, Mundi Pharma, Novartis, Pfizer and Roche (paid to institution, outside the submitted work). Travel support from Amgen, Pfizer, Roche and Teva.

No other potential conflicts of interest relevant to this article exist.

FINANCIAL SUPPORT

Marleen Keyaerts and Tony Lahoutte are Senior Clinical Investigators of the Research Foundation–Flanders (FWO). Francois Duhoux received a postdoctoral clinical mandate (2017-034) from the not-for-profit organisation 'Foundation Against Cancer' (Belgium). Research was funded by Innoviris.Brussels (RBC/2014-R-75).

ACKNOWLEDGMENTS

The authors would like to thank study coordinator Yasmine De Maeyer, nurses and technologists Gratienne Van Holsbeeck, Wendy Kemps, Nadine Eersels, Kathleen Op Debeeck, Carl Van Halewijn, Annick Luppens, Claudia Housen and Viviane Janssens for their valuable help in this trial. The authors would like to thank Peter Covens and Frank De Geeter as member of the Data Safety Monitoring Board.

KEY POINTS

QUESTION: ^{131}I-GMIB-Anti-HER2-VHH1: a candidate for HER2-targeted radionuclide therapy in breast cancer patients?

PERTINENT FINDINGS: ^{131}I-GMIB-Anti-HER2-VHH1 was found to be safe, stable after administration and rapidly cleared from blood in healthy volunteers. The tracer accumulates in metastatic sites of patients with stage IV HER2-positive breast cancer.

IMPLICATIONS FOR PATIENT CARE: Because of its favorable toxicity profile and its uptake in HER2-positive lesions, this radiopharmaceutical can offer new therapeutic options to patients who have progressed on trastuzumab, pertuzumab or T-DM1, given its difference in mode-of-action.

REFERENCES

1. Krasniqi A, D'Huyvetter M, Devoogdt N, et al. Same-day imaging using small proteins: Clinical experience and translational prospects in oncology. *J Nucl Med*. 2018 Jun;59:885-891.
2. Lecocq Q, De Vlaeminck Y, Hanssens H, et al. Theranostics in immuno-oncology using nanobody derivatives. *Theranostics*. 2019. 9:7772-7791.
3. D'Huyvetter M, Aerts A, Xavier C, et al. Development of 177Lu-nanobodies for radioimmunotherapy of HER2-positive breast cancer: evaluation of different bifunctional chelators. *Contrast Media Mol Imaging*. 2012;7:254-64.
4. Lemaire M, D'Huyvetter M, Lahoutte T, et al. Imaging and radioimmunotherapy of multiple myeloma with antiidiotypic nanobodies. *Leukemia*. 2014;28:444-7.
5. D'Huyvetter M, Vincke C, Xavier C, et al. Targeted radionuclide therapy with a 177Lu-labeled anti-HER2 nanobody. *Theranostics*. 2014;4:708-20.
6. Krasniqi A, D'Huyvetter M, Xavier C, et al. Theranostic radiolabeled anti-CD20 sdAb for targetd radionuclide therapy of Non-Hodgkin Lymphoma. *Mol Cancer Ther*. 2017;16:2828-39.
7. Bolli E, D'Huyvetter M, Murgaski A, et al. Stromal-targeting radioimmunotherapy mitigates the progression of therapy-resistant tumors. *J Control Release*. 2019;314:1-11.
8. Puttemans J, Dekempeneer Y, Eersels JL, et al. Preclinical targeted alpha and beta- -radionuclide therapy in HER2-positive brain metastasis using camelid single-domain antibodies. *Cancers*. 2020;12:1017
9. Vaneycken I, Devoogdt N, Van Gassen N, et al. Preclinical screening of anti-HER2 nanobodies for molecular imaging of breast cancer. *FASEB J*. 2011;25:2433-46.

10. Lin NU, Winer EP. Brain metastases: The HER2 paradigm. *Clin Cancer Res*. 2007;13:1648–1655.
11. Xavier C, Vaneycken I, D'huyvetter M, et al. Synthesis, preclinical validation, dosimetry, and toxicity of 68Ga-NOTA-anti-HER2 Nanobodies for iPET imaging of HER2 receptor expression in cancer. *J Nucl Med*. 2013;54:776-84.
12. Keyaerts M, Xavier C, Heemskerk J, et al. Phase I study of 68Ga-HER2-Nanobody for PET/CT assessment of HER2 expression in breast carcinoma. *J Nucl Med*. 2016;57:27–33.
13. D'Huyvetter M, De Vos J, Xavier C, et al. 131I-labeled anti- HER2 Camelid sdAb as a theranostic tool in cancer treatment. Clinical Cancer Research. 2017;23:6616-6628
14. Seret A, Nguyen D, Bernard C. Quantitative capabilities of four state-of-the-art SPECT-CT cameras. *EJNMMI Res*. 2012;2:45.
15. D'Huyvetter M, Xavier C, Caveliers V, et al. Radiolabeled nanobodies as theranostic tools in targeted radionuclide therapy of cancer. *Expert Opin Drug Deliv*. 2014;18:1-16.
16. Debie P, Lafont C, Defrise M, et al. Size and affinity kinetics of nanobodies influence targeting and penetration of solid tumours. *J Control Release*. 2019;317:34-42.
17. Pruszynski M, Koumarianou E, Vaidyanathan G, et al. Improved tumor targeting of anti-HER2 nanobody through N-succinimidyl 4-guanidinomethyl-3-iodobenzoate radiolabeling. *J Nucl Med.* 2014;55:650-6
18. Xavier C, Blykers A, Vaneycken I, et al. 18F-nanobody for PET imaging of HER2 overexpressing tumors. Nucl Med Biol 2016;43:247-52
19. Santoro L, Mora-Ramirez E, Trauchessec D, et al. Implementation of patient dosimetry in the clinical practice after targeted radiotherapy using 177Lu-[DOTA0, Tyr3]-octreotate. *EJNMMI Res*. 2018;8:103

20. Gainkam LO, Caveliers V, Devoogdt N, et al. Localization, mechanism and reduction of renal retention of technetium-99m labeled epidermal growth factor receptor-specific nanobody in mice. *Contrast media Mol Imaging*. 2011;6:85-92.
21. Marquez BV, Ikotun OF, Zheleznyak A, et al. Evaluation of 89Zr-pertuzumab in breast cancer xenografts. *Mol Pharm*. 2014;11:3988–95.

TABLES

Table 1. Mean organ doses and mean effective dose of 6 healthy subjects

Target organ	Dosimetry (male) Mean absorbed dose (mGy/MBq)	Dosimetry (female) Mean absorbed dose (mGy/MBq)
Adrenals	0.057 ± 0.016	0.074 ± 0.020
Brain	0.008 ± 0.003	0.010 ± 0.003
Breasts	0.022 ± 0.012	0.029 ± 0.016
Gallbladder wall	0.051 ± 0.015	0.061 ± 0.019
LLI wall	0.479 ± 0.061	0.521 ± 0.067
Small intestine	0.046 ± 0.017	0.057 ± 0.020
Stomach wall	0.037 ± 0.016	0.046 ± 0.020
ULI wall	0.041 ± 0.016	0.053 ± 0.021
Heart wall	0.051 ± 0.014	0.062 ± 0.018
Kidneys	1.50 ± 0.25	1.63 ± 0.27
Liver	0.127 ± 0.038	0.168 ± 0.050
Lungs	0.074 ± 0.009	0.095 ± 0.012
Muscle	0.031 ± 0.014	0.039 ± 0.018
Ovaries		0.069 ± 0.021
Pancreas	0.049 ± 0.016	0.061 ± 0.021
Red marrow	0.032 ± 0.013	0.038 ± 0.015
Osteogenic cells	0.052 ± 0.029	0.069 ± 0.038
Skin	0.022 ± 0.012	0.028 ± 0.015
Spleen	0.050 ± 0.016	0.062 ± 0.021
Testes	0.032 ± 0.014	
Thymus	0.026 ± 0.014	0.033 ± 0.018
Thyroid	0.160 ± 0.048	0.193 ± 0.059
Urinary bladder wall	0.764 ± 0.012	1.04 ± 0.01
Uterus		0.074 ± 0.021
Total body	0.042 ± 0.014	0.053 ± 0.018
	Effective Dose Whole Body (mSv/MBq)	
	0.174 ± 0.019	0.212 ± 0.022

LLI = Lower large intestines; ULI = Upper large intestines. Values are expressed as mean ± standard deviation (n=6)

FIGURES

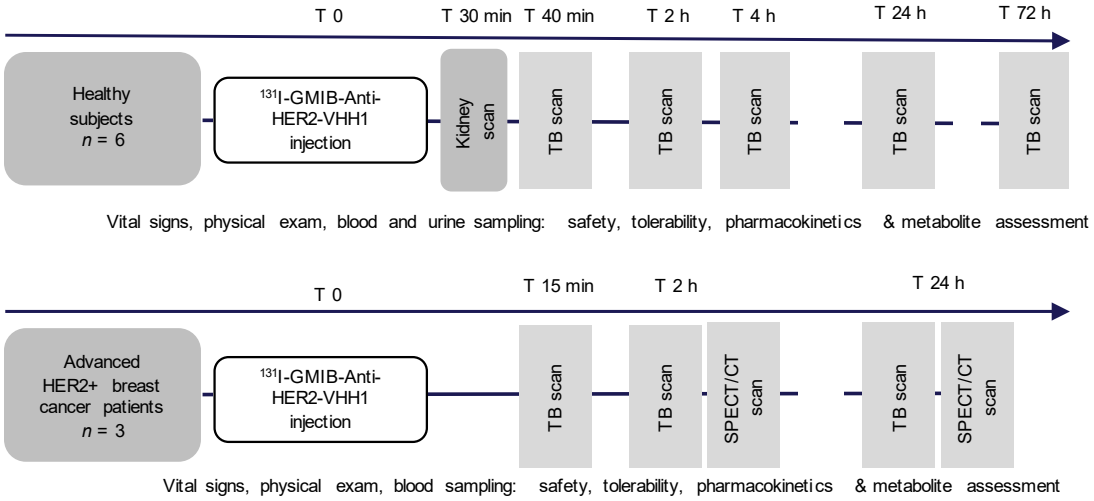

FIGURE 1. **Clinical trial design**. TB: Total body, T: Time, SPECT/CT: single photon emission computed tomography / computed tomography.

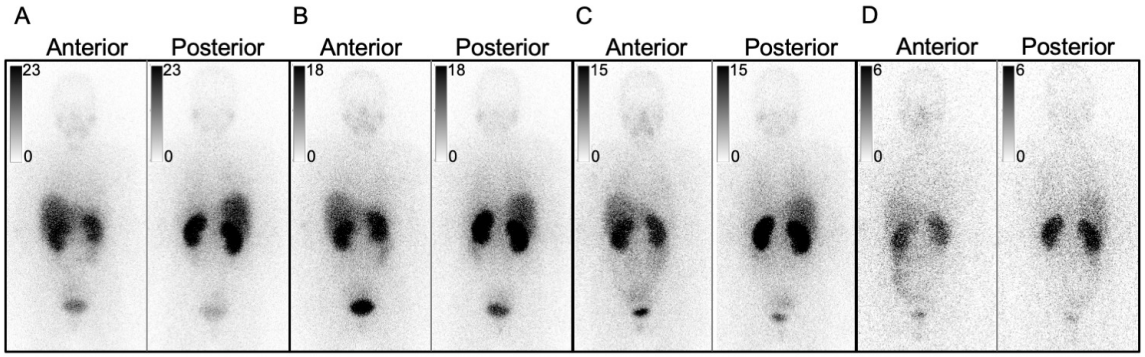

FIGURE 2. Biodistribution of ^{131}I-GMIB-Anti-HER2-VHH1 in healthy volunteer subject 3 after (A) 40 min; (B) 2 h; (C) 4 h; (D) 24 h. Anterior and posterior images from skull to thighs are displayed per time point. Images for time point 72 h only showed faint kidney and bladder activity, and were therefore omitted. Images were individually scaled (inverted gray scale expressed in counts per pixel) to allow maximal visualization of distribution at each time point. Uptake intensity is moderate throughout the time points in kidneys and liver, and low for salivary glands. An increasing level of large bowel activity could indicate a low level of intestinal clearance.

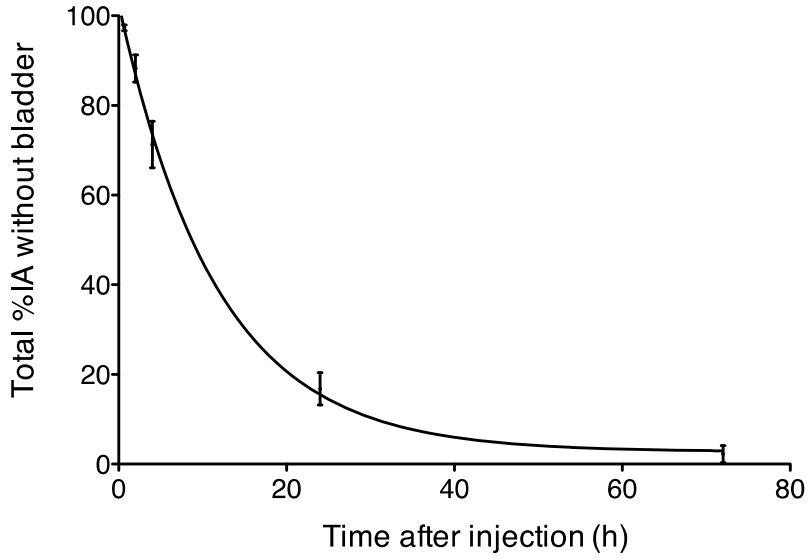

FIGURE 3. Total body clearance of ^{131}I-GMIB-Anti-HER2-VHH1 in healthy subjects. Data shown is without urinary activity present in the bladder.

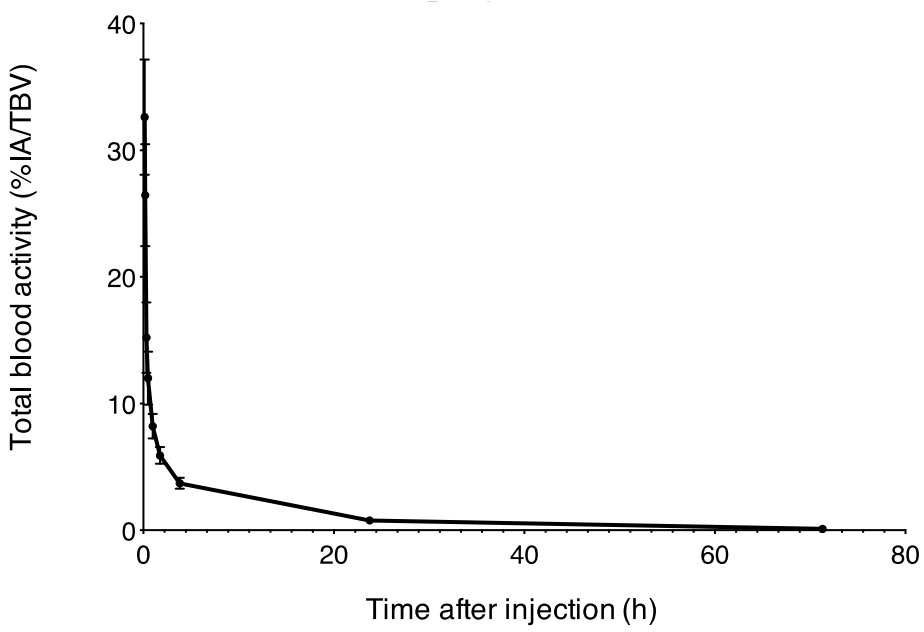

FIGURE 4. Blood clearance of ^{131}I-GMIB-Anti-HER2-VHH1 in healthy subjects. Data shown represent mean ± SD for total blood activities of 6 subjects.

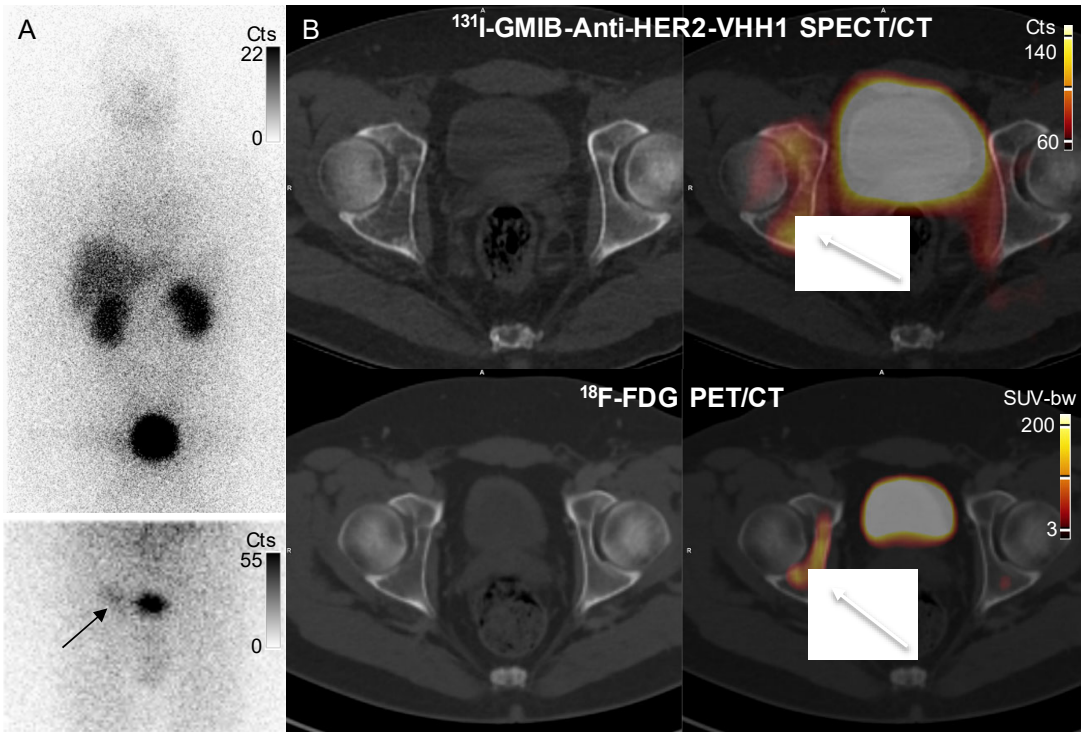

FIGURE 5. Images of uptake in bone metastasis in patient 1. A. Anterior planar whole body image 2 h after injection with pronounced bladder activity above and static anterior image over pelvis after bladder voiding below, showing moderate tracer uptake lateral of the urinary bladder. B. SPECT/CT (top) and PET/CT images at 2.5 h after ^{131}I-GMIB-Anti-HER2-VHH1 injection and 1 h after ^{18}F-FDG injection respectively, showing increased uptake in right acetabular bone (white arrow) as well as bladder activity (urinary excretion). ^{18}F-FDG-PET/CT images were obtained 44 days prior to ^{131}I-GMIB-Anti-HER2-VHH1 injection.

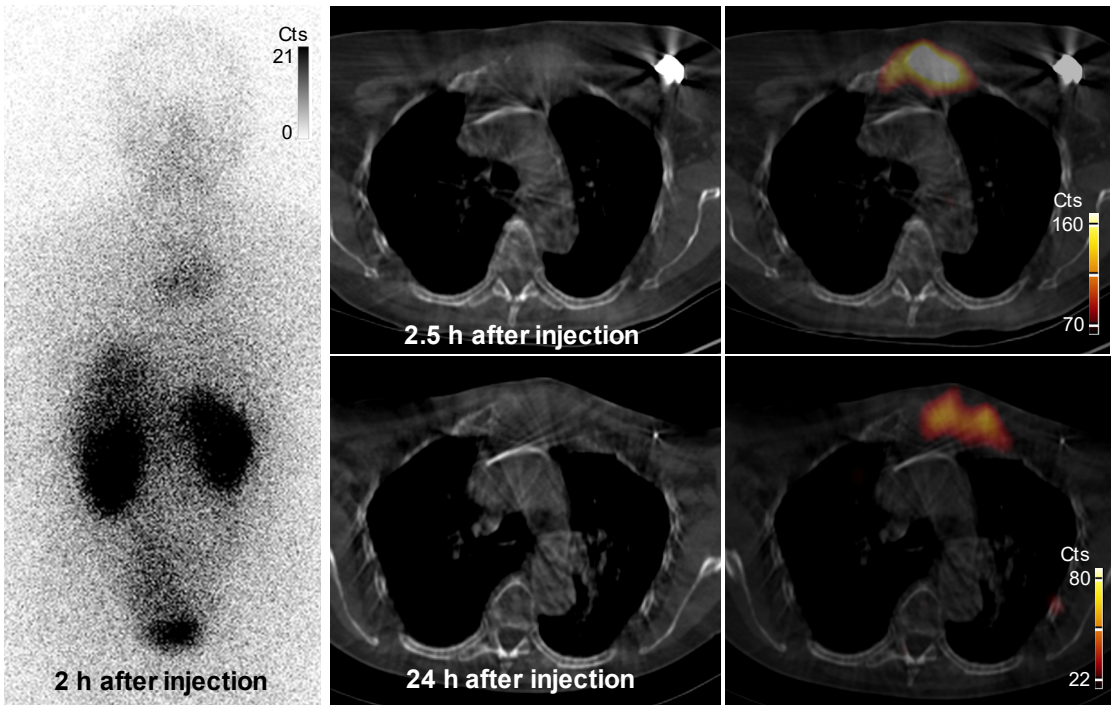

FIGURE 6. Images of uptake in bone metastasis in patient 2. Anterior whole body and SPECT/CT images showing uptake of ^{131}I-GMIB-Anti-HER2-VHH1 at the level of a large lytic bone metastasis with soft tissue component at the sternal bone both at 2.5 h and at 24 h after injection. Small differences in area of the uptake are explained by differences in patient positioning (arms up at 2.5 h and arms down at 24 h, to maximize patient comfort).

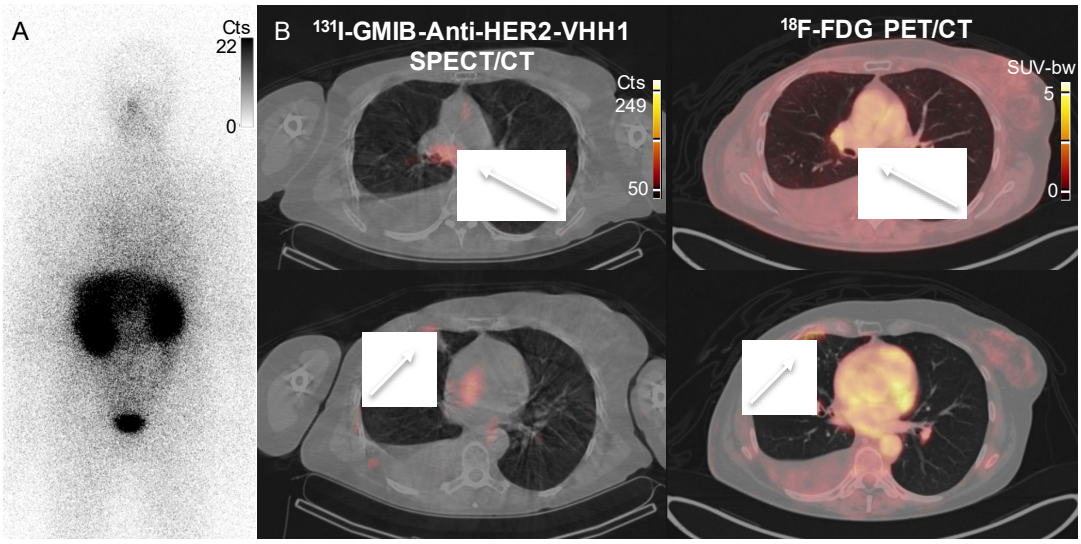

FIGURE 7. Images of patient 3 showing metabolically-active sites of disease at subcarinal lymph node and pleural metastasis. A. Anterior whole-body planar image at 2 h after injection showing no focal uptake in thoracic region. B. Uptake of ^{131}I-GMIB-Anti-HER2-VHH1 at 2.5 h after injection is weak and close to background activity in subcarinal lymph node of 13 mm.

GRAPHICAL ABSTRACT

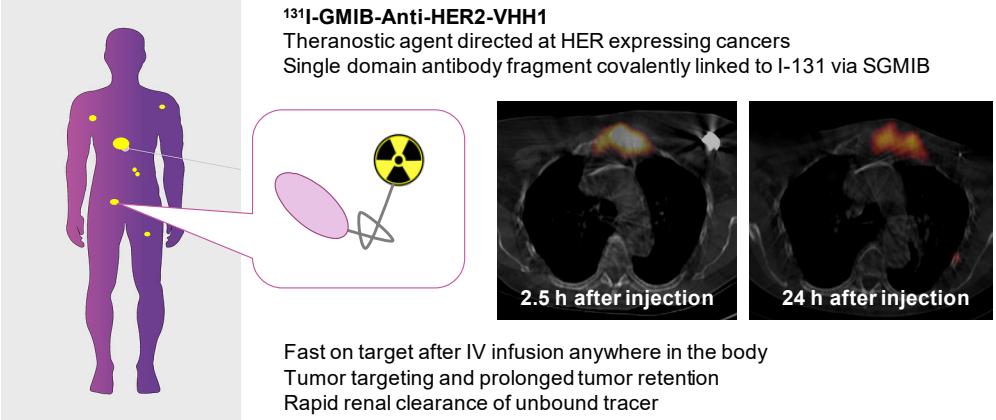

^{131}I-GMIB-Anti-HER2-VHH1
Theranostic agent directed at HER expressing cancers
Single domain antibody fragment covalently linked to I-131 via SGMIB

Fast on target after IV infusion anywhere in the body
Tumor targeting and prolonged tumor retention
Rapid renal clearance of unbound tracer

Phase I trial of ^{131}I-GMIB-Anti-HER2-VHH1, a new promising candidate for HER2-targeted radionuclide therapy in breast cancer patients

SUPPLEMENTAL TABLES

SUPPLEMENTAL TABLE 1. Subject demographics

Healthy subjects (n = 6)	**Mean (range)**
Age (y)	29.5 (23-47)
Height (cm)	171.7 (163-180)
Mass (kg)	68.3 (53-100)
BMI (kg/m^2)	23.0 (19.0-30.9)
Sex	5 females / 1 male
Ethnicity	
Caucasian	100%
Patients (n = 3)	**Mean (range)**
Age (y)	60.3 (43-77)
Height (cm)	161.7 (145-171)
Mass (kg)	66.0 (51-88)
BMI (kg/m^2)	25.0 (20.7-30.1)
Sex	2 female / 1 male
Ethnicity	
Caucasian	100%

BMI = body mass index

SUPPLEMENTAL TABLE 2. Biodistribution of ^{131}I-GMIB-VHH1 in healthy volunteers after 40 min, 2 h, 4 h, 24 h and 72 h. Data are presented as % injected activity through a mean value (n = 6) ± SD.

	40 min			2 h			4 h			24 h			72 h		
Target organ	**mean**	**±**	**SD**	**mean**	**±**	**SD**	**mean**	**±**	**SD**	**mean**	**±**	**SD**	**mean**	**±**	**SD**
Brain	0.21	±	0.06	0.20	±	0.06	0.18	±	0.04	0.06	±	0.03	0.004	±	0.002
Thyroid	0.23	±	0.05	0.18	±	0.05	0.15	±	0.04	0.03	±	0.01	0.002	±	0.001
Lung	4.20	±	0.39	3.56	±	0.33	2.87	±	0.21	0.54	±	0.12	0.04	±	0.01
Heart	1.27	±	0.09	1.05	±	0.07	0.80	±	0.04	0.15	±	0.02	0.01	±	0.002
Liver	14.43	±	5.68	10.62	±	4.36	7.96	±	3.28	1.52	±	0.47	0.10	±	0.02
Kidneys	24.30	±	2.31	21.75	±	2.13	17.86	±	2.18	4.35	±	0.98	0.32	±	0.10
Lower large Intestine	6.78	±	0.99	7.14	±	0.96	5.49	±	0.88	2.04	±	2.12	0.13	±	0.08
Bladder	2.70	±	0.67	5.10	±	1.53	1.77	±	0.31	0.27	±	0.05	0.14	±	0.17
Muscle	0.01	±	0.001	0.01	±	0.001	0.004	±	0.001	0.001	±	0.0004	0.0002	±	0.0003
Whole body	100.00	±	0.00	92.91	±	2.45	72.19	±	4.92	15.74	±	3.32	1.88	±	1.44
Whole body remainder	45.88	±	4.86	43.32	±	4.33	35.11	±	3.96	6.79	±	3.80	1.14	±	1.30

SUPPLEMENTAL FIGURES

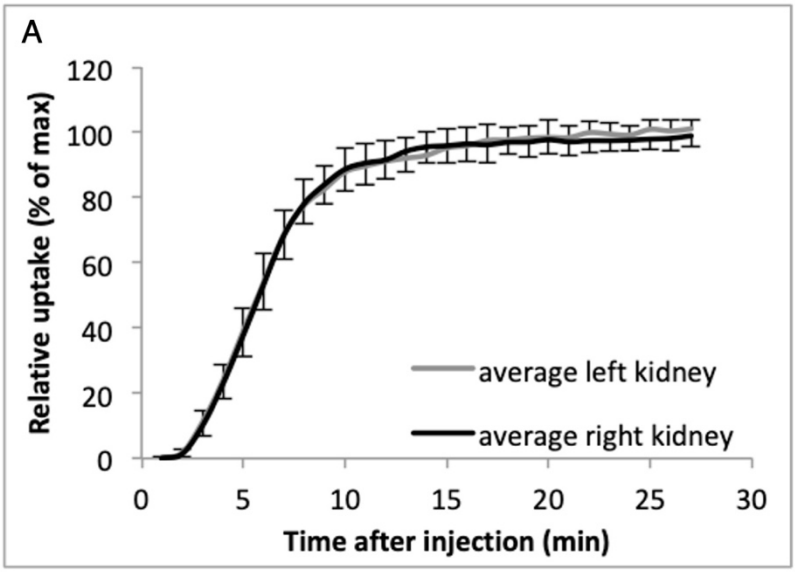

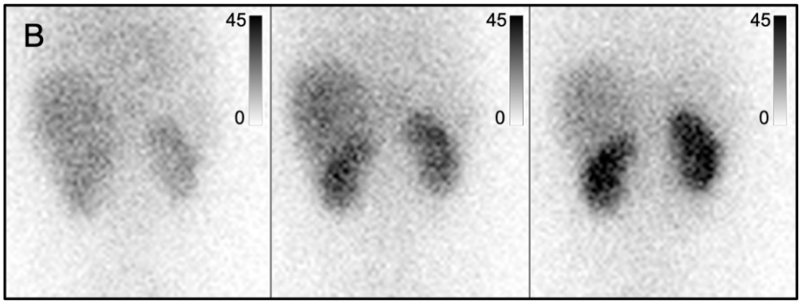

SUPPLEMENTAL FIGURE 1. Dynamic kidney activity in healthy volunteers between injection and 30 min after injection. (A) Average activity in left and right kidney over 6 subjects, expressed as % of uptake at the end of the dynamic acquisition. (B) Representative images of subject 6 at end of administration (5-6 min, left), at 9-10 min (middle) and at 29-30 min (right), equally scaled and expressed in counts/pixel.

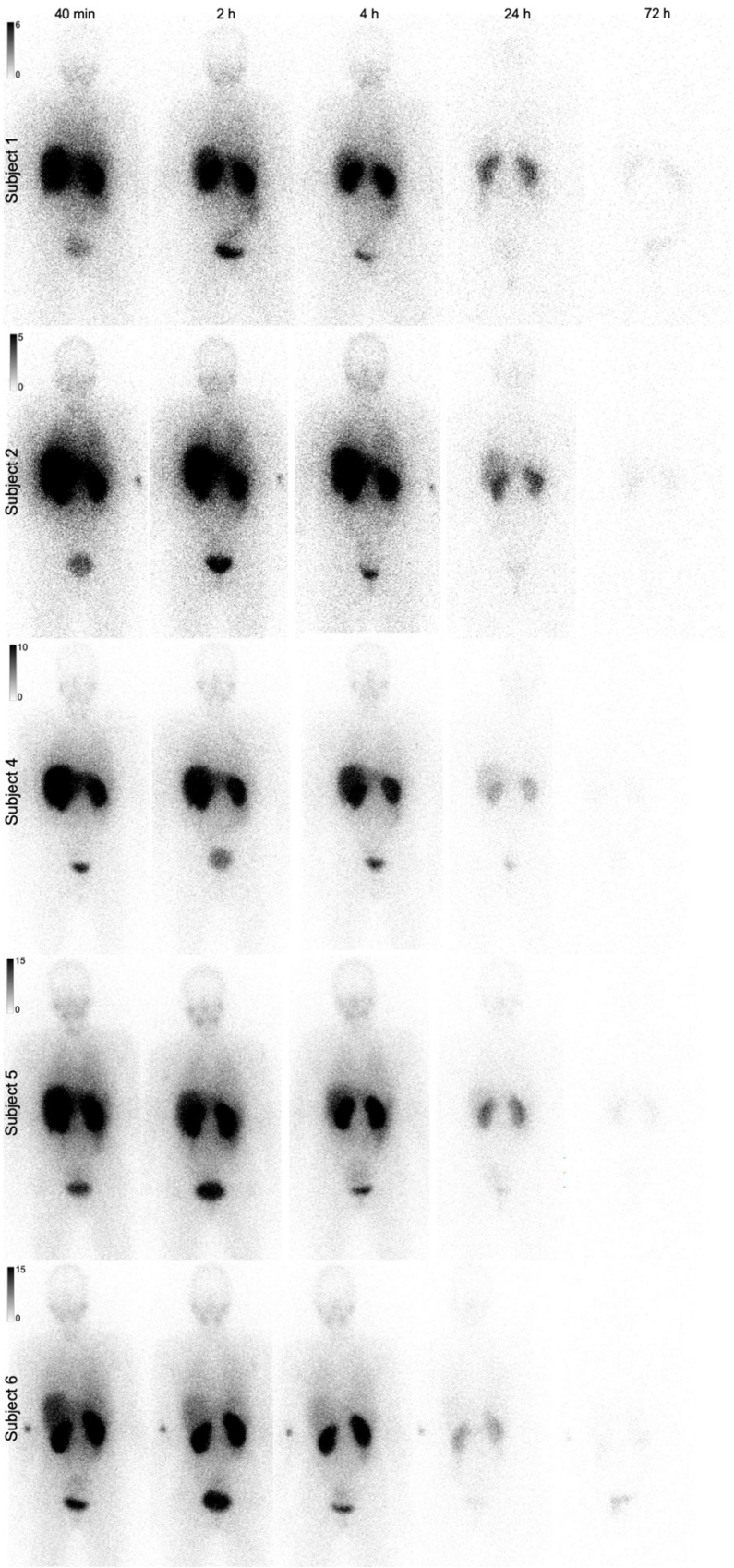
40 min
2 h
4 h
24 h
72 h
6
0
Subject 1
5
0
Subject 2
10
0
Subject 4
15
0
Subject 5
15
0
Subject 6

SUPPLEMENTAL FIGURE 2. Whole body biodistribution in healthy volunteers. Images are presented as geometric mean and equally scaled (expressed in counts per pixel and decay c

orrected) per subject.

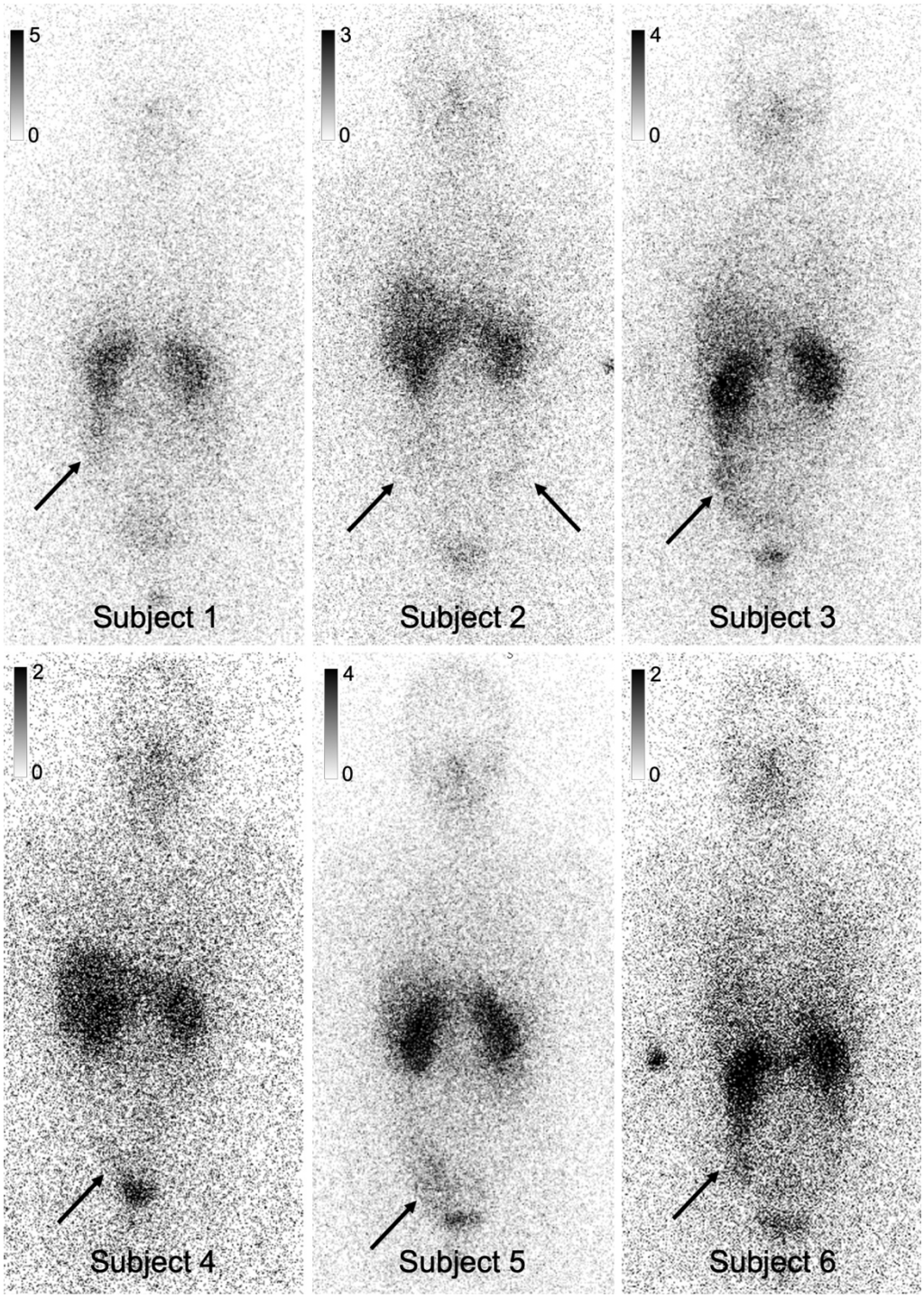

SUPPLEMENTAL FIGURE 3. Anterior planar images of healthy subjects showing tracer accumulation in large bowel. Images at 24h after injection. Arrows indicate accumulation of low intensity over the large bowel area, indicating a low level of gastro-intestinal activity of the radiopharmaceutical.